

# Synergistic effect of carbon nanotube and clay for improving the flame retardancy of ABS resin

Haiyun Ma<sup>1</sup>, Lifang Tong<sup>1</sup>, Zhongbin Xu<sup>1</sup> and Zhengping Fang<sup>1,2,3</sup>

<sup>1</sup> Institute of Polymer Composites, Key Laboratory of Macromolecular Synthesis and Functionalization, Zhejiang University, Hangzhou 310027, People's Republic of China

<sup>2</sup> Department of Biochemical and Chemical Engineering, Ningbo Institute of Technology, Zhejiang University, Ningbo 315100, People's Republic of China

E-mail: [zpfang@zju.edu.cn](mailto:zpfang@zju.edu.cn)

Received 5 March 2007, in final form 21 July 2007

Published 22 August 2007

Online at [stacks.iop.org/Nano/18/375602](http://stacks.iop.org/Nano/18/375602)

## Abstract

Synergistic effect between multi-walled carbon nanotubes (MWNTs) and clay on improving the flame retardancy of acrylonitrile–butadiene–styrene (ABS) resin was studied. Flammability properties measured by a cone calorimeter revealed that incorporation of clay and MWNTs into ABS resin significantly reduced the peak heat release rate (PHRR) and slowed down the whole combustion process compared to the individually filled system based on clay or MWNTs. The flame retardancy of the ABS/clay/MWNTs nanocomposites was strongly affected by the formation of a network structure. Linear viscoelastic properties of the ABS nanocomposites showed that the coexistence of clay and MWNTs can enhance the network structure which can hinder the movement of polymer chains and improve flame retardancy. From transmission electron microscope analysis, MWNTs were shortened after combustion and there was no significant change in their diameters. For chars of ABS/clay/MWNTs nanocomposites, some MWNTs ran across between clay layers, indicating a strong interaction existed between clay and MWNTs. The existence of clay enhanced the graphitization degree of MWNTs during combustion. Clay can assist the elimination of dislocations and defects and the rearrangement of crystallites. Al<sub>2</sub>O<sub>3</sub>, one of the components of clay, acts as the catalyst of graphitization.

## 1. Introduction

Much attention has been attracted in using carbon nanotubes (CNTs) for making polymer nanocomposites in recent years due to their excellent properties [1–5]. One such example is to modify the flammability properties of polymers with CNTs. Kashiwagi *et al* [6–9] investigated the flammability of polypropylene (PP)/multi-walled carbon nanotube (MWNTs) nanocomposites. They reported that the observed flame-retarded performance of the PP/MWNTs nanocomposite is mainly due to chemical and/or physical processes in the condensed phase instead of in the gas phase. The MWNTs form network structured layers in the PP matrix.

Such network layers shield the PP resin from external radiation and heat feedback from flame and also act as excellent thermal insulation layers. Scharrel *et al* reached similar conclusions after the investigation of polyamide-6(PA-6)/MWNTs nanocomposites [10].

Organoclay is another commonly used nanoscale filler for flame retarding of polymers due to its excellent barrier effect [11–15]. Several important review articles [16–18] have been published recently on the flammability of polymer/clay nanocomposites. The synergistic effect between CNT and organoclay in flame retarding performance was also investigated in recent years [19–23]. The synergistic mechanism was generally explained in that CNT acts as a sealing agent that can connect clay layers and reduce surface cracks of chars, leading to the increase of barrier resistance to

<sup>3</sup> Author to whom any correspondence should be addressed.

the evolution of flammable volatiles and oxygen ingress to the condensed phase.

Most of the previous studies on polymer nanocomposites in the field of flame retardation focused on the relationship between the macroscopic morphologies of chars and the flammability properties [11–15]. However, more work should be done on the relationship between evolution of the microstructure, viscoelasticity and graphitization degree of chars and the flammability of polymers during combustion. Some previous studies have shown that the mechanical, thermal and friction properties are significantly affected by the variation of graphitization degree of carbon nanotubes [24, 25].

In this paper we present nanocomposites based on acrylonitrile–butadiene–styrene resin (ABS), clay and MWNTs directly blended in the melt state. Our attention is focused on the influences of the mesoscopic filler network and graphitization degree of chars on the flammability of ABS resin. The mechanism of the synergistic effect between clay and carbon nanotubes on improving the flame retardancy is discussed.

## 2. Experimental details

### 2.1. Materials

MWNTs were provided by the Institute of Material Physics and Microstructure at Zhejiang University (China) and prepared by the catalytic decomposition of acetylene at 700 °C for ca. 60 min [26]. The average diameter of MWNTs is 30–80 nm which was measured by transmission electron microscopy (TEM). Organically modified clay (Na<sup>+</sup>-montmorillonite) was supplied by Zhejiang Huate Clay Products of China, which was ion-exchanged with octadecyl trimethyl ammonium bromide (C<sub>18</sub>). The cation exchange capacity (CEC) of the clay was 98 mequiv/100 g. ABS resin (HI-121H) was obtained from LG Industries, Korea.

### 2.2. Preparation of ABS/clay/MWNTs nanocomposites

Composites containing various clay and MWNTs content were prepared via melt compounding at 190 °C in ThermoHaake Rheomix with a screw speed of 60 rpm, and the mixing time was 10 min for each sample. The mixed samples were transferred to a mold and preheated at 190 °C for 3 min, then pressed at 14 MPa, and successively cooled to room temperature while maintaining the pressure to obtain composite sheets for further measurements.

### 2.3. Measurements and characterization

Flammability of the nanocomposites was characterized using a cone calorimeter performed in duplicate with an FTT, UK device according to ISO 5660 at an incident flux of 35 kW m<sup>-2</sup> using a cone-shaped heater. The data reported here are the averages of three replicated experiments. Rheology measurements were performed using an ARES rotational rheometer (Rheometrics, Inc.) with a parallel plate geometry (plate diameter = 25 mm, gap = 1.5 mm) in air. Dynamic frequency sweep tests were executed in the frequency range of 0.01–100 rad s<sup>-1</sup>. Dynamic temperature sweep tests were executed in the temperature range of 180–300 °C with a heating rate of 10 °C min<sup>-1</sup> at 0.1 rad s<sup>-1</sup> (low shear simulating

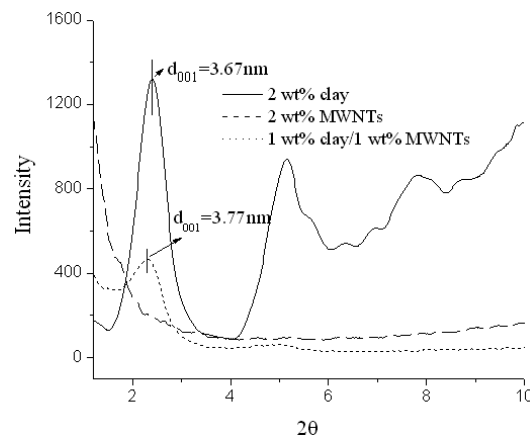


Figure 1. XRD patterns of ABS nanocomposites.

burning condition of the sample). Morphological studies of the dispersion of MWNTs and clay in the matrix were performed using a field emission scanning electron microscope (FESEM, FEI Sirion) and a transmission electron microscope (TEM, JEM-1200EX). Morphology of the char residues after cone calorimeter tests was investigated by FESEM and optical microscopy (OM). The graphitization degree of MWNTs and the resultant composites were determined using x-ray diffraction (XRD) analysis (Rigaku, Japan) with Cu K $\alpha$  radiation (0.15416 nm) and Raman spectrometer (Thermo Nicolet, USA) using a Ar-ion laser excitation (732 nm, 5 mW, resolution 1 cm<sup>-1</sup>). The position and width of the peaks of XRD were calibrated with respect to a silicon internal standard. The interlayer spacing ( $d_{002}$ ) was calculated from the Bragg and Scherrer equations, respectively [27]. The graphitization degree was calculated from Maire and Mering's equation [28, 29].

## 3. Results and discussion

### 3.1. Dispersion of clay and carbon nanotubes

The distribution of the clay and MWNTs in the composites was examined by XRD (figure 1) and TEM (figures 2(a)–(c)). The main peaks correspond to the (001) plane reflections of the clays. The (001) diffraction of clay was at  $2\theta = 4.65^\circ$ , corresponding to an interlayer spacing of 1.92 nm from our previous report [30]. For the ABS/clay composites, the characteristic (001) peak of the clay was shifted to  $2\theta = 2.42^\circ$  (corresponding to a basal spacing of 3.67 nm), indicating an intercalated structure was formed. For the sample of ABS/clay/MWNTs nanocomposites, the position of (001) peak slightly decreases and the basal spacing ( $d_{001} = 3.77$  nm) is 0.1 nm larger compared to ABS/clay nanocomposites. The peak intensity decreases significantly and peak broadness increases, suggesting a better dispersion of clay for the ABS/clay/MWNTs nanocomposites than that of the ABS/clay sample. Compared to XRD profiles, TEM images show the visualized impression for the dispersion of clay and MWNTs in composites. A TEM micrograph for ABS/clay nanocomposites (figure 2(a)) shows that the clay layers consist of highly oriented multilayered stacks, about 20–100 nm in

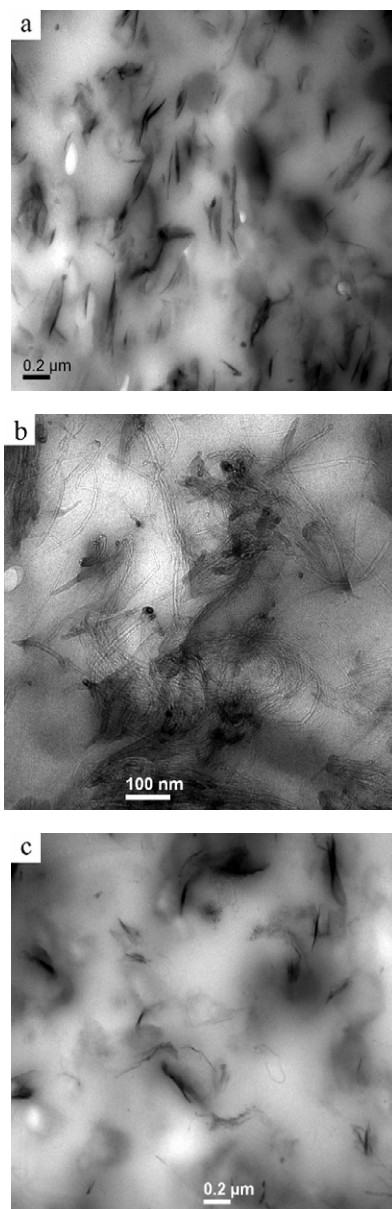


**Figure 2.** The dispersion of clay and MWNTs in nanocomposites: ABS/2%clay (a) ABS/2%MWNTs (b) ABS/1%clay/1%MWNTs (c).

composites. No individual silicate layers were seen in the composites and it indicates that no exfoliation occurred in the composites. Figure 2(b) shows the dispersion of MWNTs in the ABS matrix. Regions of slight nanotube aggregation and tubes with a curled, entangled structure were observed. For ABS/clay/MWNTs sample (figure 2(c)), there is a better dispersion of clay and some disordered single platelets can be seen in the TEM image. On the basis of the above-mentioned TEM and XRD results, it is possible to deduce that some MWNTs were intercalated into the clay galleries and the composite formed a mixed intercalated/delaminated structure.

### 3.2. Flammability properties

A cone calorimeter was used to evaluate the fire properties of the system. During the cone experiments, visual observations

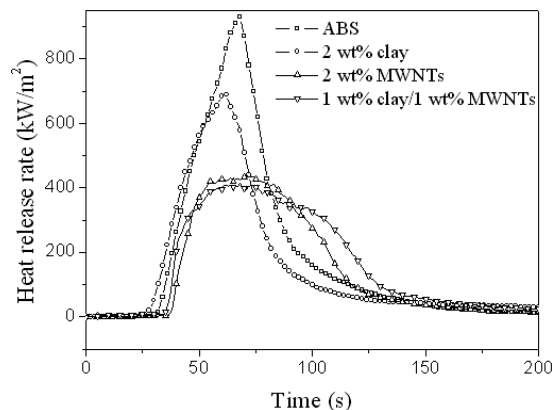


**Figure 3.** Heat release rate versus time measured with a cone calorimeter (heat flux:  $35 \text{ kW m}^{-2}$ ) for ABS nanocomposites.

reveal different fire behavior for pure ABS and ABS/MWNTs composites. As expected, the pure ABS resin melted and behaved like a liquid accompanied by numerous bubbles bursting on the sample surface. At the end of the test, no residue was left, confirming the poor carbonization effect of ABS. On the other hand, all the nanocomposites behaved like a solid without obvious melting. For ABS/clay and ABS/MWNTs nanocomposites, black discrete islands formed and thin char grew with a tendency for cracking between them during combustion. But for ABS/clay/MWNTs nanocomposites, a relatively intact char layer was left compared to ABS/clay or ABS/MWNTs ones. A more detailed explanation of this phenomenon is given in the following sections.

A comparison of heat release rate curves of ABS resin and its nanocomposites is shown in figure 3. It is evident from the results that all the nanocomposites had improved flame retardant properties and MWNTs were more effective in the reduction of peak heat release rate (PHRR) than clay. The synergistic effect exists between clay and MWNTs for flame retardancy, which is consistent with the previous reports [19]. The different aspect is that not only the PHRR was reduced but also the whole combustion process was slowed down compared to the individually filled system. Although the coexistence of clay and MWNTs can reduce the flammability of the nanocomposites more efficiently than the individual component (clay or MWNTs) filled samples in the measurement by cone calorimeter, ABS/clay/MWNTs nanocomposites still failed to pass the traditional flame retardancy such as the UL 94 test. The comprehensive review by Morgan [16] shows that a flame retardant nanocomposite considered to be a regulatory 'pass' does not necessarily have the same flammability performance when compared to another material at the same regulatory 'pass' level. The synergistic effect between clay and MWNTs still has its significance in improving flame retardancy of materials and is worthy to be further studied.

Combustion is a very complex physical and chemical process that is determined by many factors such as viscoelasticity and the structure of chars formed during combustion. The following investigations were focused on the characterization of rheological properties and the char's structure.

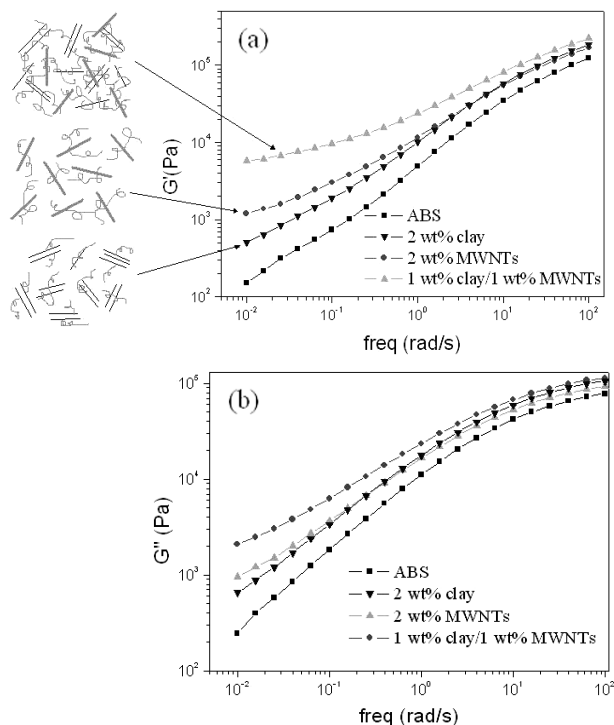


**Figure 4.** Linear melt-state rheological properties as a function of oscillatory frequency: (a) storage modulus,  $G'$  and (b) loss modulus,  $G''$ .

### 3.3. Evidence of the network structure and its effects on flammability properties

For the clay or carbon nanotubes filled nanocomposites, it was proposed that a so-called three-dimensional filler network structure will form when the content of layered clay reaches a threshold value [31]. The threshold value was determined by the dispersion of the nanoparticles [32–38]. The construction of a nanoparticle network can be demonstrated by the change of dynamic melt rheological properties. Figure 4 shows the storage modulus ( $G'$ ) (figure 4(a)) and loss modulus ( $G''$ ) (figure 4(b)) of the ABS and ABS/clay/MWNTs nanocomposites at 200 °C. In the high  $\omega$  regime corresponding to the movement within a small timescale, not much difference in  $G'$  is seen for the nanocomposites with different samples, which implied that the movements of partial polymer chains were not affected by the addition of clay and MWNTs. However, the  $G'$  in the low  $\omega$  regime is significantly dependent on the addition of clay and MWNTs. The rheological properties in the low  $\omega$  regime can be regarded to reflect the relaxation and motion of the whole polymer chains. From the results of figure 4, it is observed that the terminal slope of  $G'-\omega$  curves decreases with the addition of clay and MWNTs compared to pure ABS resin, indicating a percolated filler network is established in which the free movement of ABS chains is restricted by the spatially confined geometry. The minimal value of the terminal slope of  $G'-\omega$  curves is found in ABS/clay/MWNTs nanocomposites which indicates a more intact percolated network structure formed in ABS/clay/MWNTs nanocomposites than in ABS/clay and ABS/MWNTs nanocomposites. The frequency dependence of

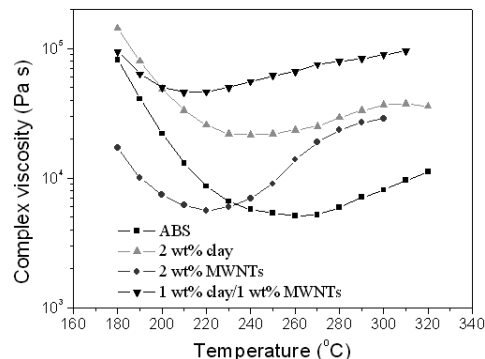


**Figure 5.** Dependence of complex viscosity on temperature for ABS nanocomposites.

$G''$  shows a similar trend. From the results of figure 4, it can be seen that the increase of the storage modulus of all samples is greater than the increase of the loss modulus. Therefore, the structure of the nanocomposites is more sensitively reflected in the storage modulus than in the loss modulus [39].

Comparing the results of dynamic frequency sweep tests and flammability properties of the materials in this study, we can conclude that the flame retardancy of polymer nanocomposites is strongly affected by the formation of the network structure which can improve the barrier resistance to the evolution of flammable volatiles and the oxygen ingress to the condensed phase. MWNTs are one-dimensional nanotubes which have a highly elongated shape (high aspect ratio) and layered silicates are one to a few nanometers in thickness and hundreds to thousands of nanometers in the other two dimensions. The coexistence of clay and MWNTs in the composites can form a more effective confined space and enhance the network structure, which can be responsible for the improved flame retardancy of the polymer nanocomposites in this study.

Figure 5 shows the temperature dependence of complex viscosity for the ABS resin and its nanocomposites with the temperature ranging from 180 to 300 °C. From the results of figure 5, it can be seen that the complex viscosity decreases and then increases with the increase of temperature. A minimum value exists within the temperature range. The minimum value appears at 270 °C for pure ABS resin and at 240 °C, 220 °C and 210 °C for ABS/clay, ABS/MWNTs and ABS/clay/MWNTs nanocomposites, respectively. The complex viscosity significantly increases with the addition of clay and MWNTs at higher temperature. For ABS/clay/MWNTs nanocomposite, the complex viscosity increases by at least one order of magnitude than pure ABS resin when the temperature is higher than 240 °C. When heated, ABS chains become easier to move then generate a decrease of complex viscosity. At a higher temperature (>270 °C), oxidation and cross-linking reactions occur among macromolecular chains, which causes the increase of complex viscosity. For the nanocomposites, the cross-linking process occurs earlier and forms a network structure than pure ABS resin due to the hindering effect of the confined geometry originating from clay and MWNTs. Because coexistence of clay and MWNTs can form a more effective confined geometry, the network structure can be constructed at lower temperature in

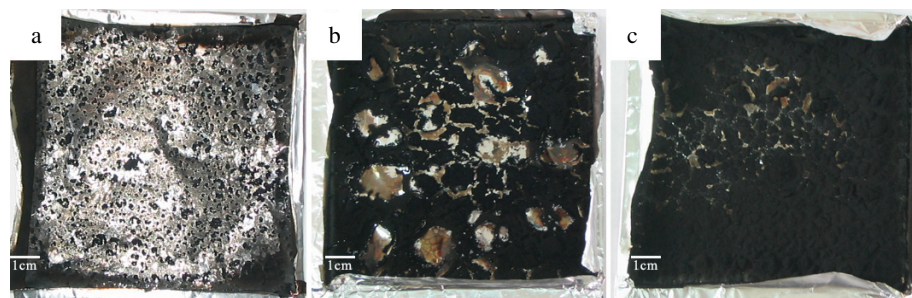


**Figure 6.** Pictures of the chars of ABS nanocomposites after cone calorimeter tests: ABS/2 wt% clay (a), ABS/2 wt% MWNTs (b), ABS/1 wt% clay/1 wt% MWNTs (c).

ABS/clay/MWNTs nanocomposites and protect the polymer matrix more efficiently.

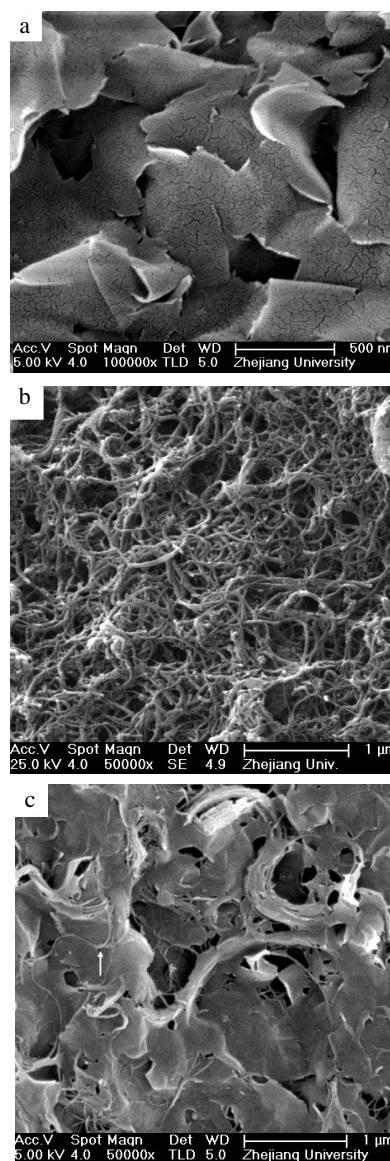
#### 3.4. Effects of char's structure on the flammability properties

Figure 6 shows the macro-morphologies of chars for the nanocomposites. A thick, relatively intact char layer with lower crack density was formed for ABS/clay/MWNTs nanocomposites (c) than the individual filled samples ((a), (b)). The detailed micro-morphologies of the samples were shown in figures 7 and 8. A tight char with some pores between the clay layers and many microcracks in the layer surface was observed for the ABS/clay sample (figure 7(a)). Consistent with the results of our previous study [30], the image of ABS/MWNTs nanocomposites shows a network structure without obvious cracks and openings, as shown in figure 7(b). The char layers of individual clay or MWNTs filler act as a heat shield to improve the flame retardant properties of ABS resin. For ABS/clay/MWNTs nanocomposites, the chars are tighter and denser and have fewer pores and microcracks than that of the individually filled sample. Some MWNTs act as the 'bridge' and overlap the pores between clay layers; other MWNTs are inlaid between clay layers and form a sandwich structure and this may be a proof of the intercalation of MWNTs into clay layers during processing. From TEM images in figure 8, it can be seen that MWNTs were shortened after combustion and there is no significant change in their diameters. For chars of ABS/clay/MWNTs nanocomposites, it is found that many MWNTs run across between clay layers, indicating a strong interaction between clay and MWNTs.

#### 3.5. Effects of the graphitization degree of chars on the flammability properties

The microstructure of chars is a critical factor for flammability properties of polymers. For a carbon-nanotube-filled flame retardant system, the degree of graphitization is a very important structural parameter, which reflects the transition extent of carbon material from a turbostratic to graphitic structure and determines the properties of the material [40]. X-ray diffraction (XRD) and Raman spectroscopy were used to investigate the graphitization degree in this work.

XRD is a traditional method to detect information about crystal structure for carbon materials. The 002 peak in the XRD profile is a synthetic reflection of all the micro-graphite crystals in carbon materials [41]. According to the Bragg



**Figure 7.** FESEM image of the chars of ABS nanocomposites after cone calorimeter tests: ABS/2 wt% clay (a), ABS/2 wt% MWNTs (b), ABS/1 wt% clay/1 wt% MWNTs (c).

equation, the interlayer spacing  $d_{002}$  can be obtained, and on the basis of the model given by Maire and Mering [28], the

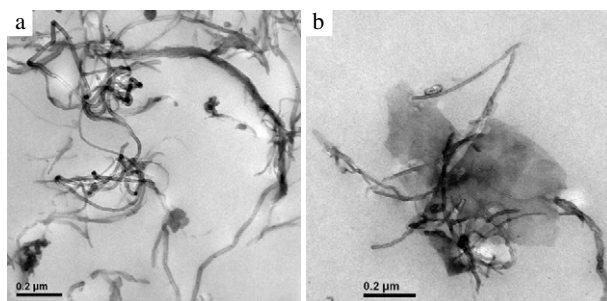


**Figure 8.** TEM image of the chars of ABS nanocomposites after cone calorimeter tests: ABS/2 wt% MWNTs (a), ABS/1 wt% clay/1 wt% MWNTs (b).

value of the graphitization degree ( $g$ ) can be calculated from the following equation:

$$g = \frac{0.3440 - d_{002}}{0.3440 - 0.3354} \times 100\%$$

where 0.3440 is the interlayer spacing of the fully non-graphitized carbon (nm), 0.3354 is the interlayer spacing of the ideal graphite crystallite and  $d_{002}$  is the interlayer spacing derived from XRD (nm) [40]. In this equation, 0.3440 nm represents a certain specific structure according to Franklin [42] who considered it as an interlayer spacing of the non-graphitic carbons. Such a restriction has its limitation because the apparent interlayer spacing of a turbostratic structure is sometimes greater than 0.3440 nm: then  $g < 0$  will be deduced from this equation. Although the negative value has no real meaning, it could be used in this paper to represent a structure that is far from the ideal graphite structure [40].

Raman spectroscopy was used to further characterize graphitization of the MWNTs. The peak at  $1600\text{ cm}^{-1}$  (G-band) corresponds to an  $E_{2g}$  mode of hexagonal graphite and is related to the vibration of  $sp^2$ -hybridized carbon atoms in a graphite layer. The D-band at about  $1360\text{ cm}^{-1}$  is associated with the vibration of carbon atoms with dangling bonds in the plane terminations of disordered graphite or glassy carbon. The ratio of the integral peak intensity of the G-band and D-band,  $R = I_G/I_D$ , representing the graphitization degree of the chars [43].

Figure 9 shows the graphitization degree of chars for the nanocomposites of this work. Results show that chars of ABS/clay/MWNTs exhibit a much higher graphitization degree than that of ABS/MWNTs. From the XRD profiles, for ABS/MWNTs nanocomposites, the sample before burning does not have a graphite structure, indicating MWNTs contain plenty of turbostratic carbons. On the other hand,  $d_{002}$  (0.3371 nm) of the chars for ABS/clay/MWNTs nanocomposites is much closer to the (002) peak of graphite than that of the ABS/MWNTs sample (0.3506). The results of Raman spectra show the same conclusion with XRD profiles. The lower degree of graphitization in the char has relatively high reactivity to oxidation, leading to the char burnt out in the long time exposure to a high extent of heat flux as occurring in the cone calorimeter [20].

It can be concluded that a higher graphitization degree in the char structure tends to give better protection of materials from thermal oxidation. But why can clay promote

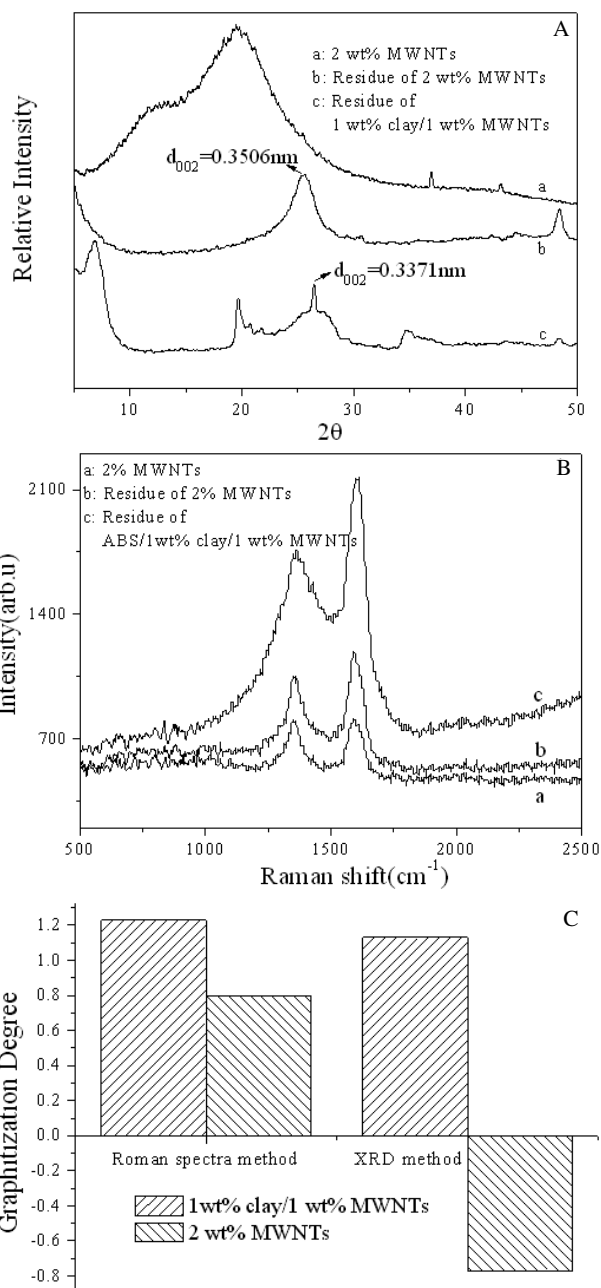
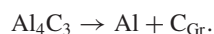
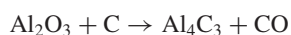


**Figure 9.** Graphitization degrees of chars of ABS nanocomposites: XRD profiles (A), Raman spectra (B), calculation results of graphitization degree from XRD profiles and Raman spectroscopy for the chars of ABS nanocomposites (C).

the formation of graphitic carbon under fire conditions? Graphitization is a converting process of a disordered structure to a perfect graphitic structure. During the processing above, basal spacing of  $d_{002}$  decreases with the increase of graphitization degree [44]. A normal relationship exists between temperature, pressure and graphitization degree. When temperature increases, a small aromatic nucleus, nonplanar  $sp^3$  cross-linked structure and some residual C–H bonds are broken and escaped. Other aromatic layers are stacked together progressively to form ordered graphitic carbons. In such a process, strong inner stress is generated

due to the anisotropic expansion of aromatic layers. The dislocations and defects in such structures were eliminated, while crystallites were rearranged and formed ordered 3D graphitic structures. The intercalated/exfoliated clay layers in the nanocomposites are believed to act as an important role during the process above. The expansive aromatic layers were blocked by the clay layers. The tight and closed connection between aromatic layers and clay layers make a more intact graphitic structure under the strong compression. Figures 7(c) and 8(b) show the tight sticking between the nanotubes and clay layers, indicated by the white arrow.

Another role of clay on the enhancement of the graphitization degree of MWNTs may be its catalytic effect. As catalysts, metals such as Fe, Si, Ti, Ca, Mg and Al, and oxides such as Al<sub>2</sub>O<sub>3</sub> and MgO were used [45–47]. The graphitization degree can be improved by using such catalysts. The clay used in this paper is montmorillonite which possesses a sandwich structure of tetrahedral–octahedral–tetrahedral aluminosilicate lamellar materials formed by condensation of an octahedral Al<sub>2</sub>O<sub>3</sub> between two tetrahedral SiO<sub>2</sub> [48]. The mechanism of graphitization of MWNTs by an Al-containing catalyst is considered to be that the aluminum compound reacted with C to give Al<sub>4</sub>C<sub>3</sub> and the Al<sub>4</sub>C<sub>3</sub> compound decomposed to Al and C<sub>Gr</sub> which was graphitized [47]:



Normally, a temperature higher than 1500 °C was needed for the graphitizing reaction mentioned above for common isotropic carbon. However, the temperature during cone calorimeter measurements in this work is only 700 °C, so the reaction mentioned above may be attributed to the size effect of carbon nanotubes and the special interlayer structure of clay. Further investigations are needed to confirm such a statement.

#### 4. Conclusions

ABS/clay/MWNTs nanocomposites were prepared by melt mixing. Synergistic effect on improving flame retardancy was found between clay and MWNTs. Flammability properties measured by a cone calorimeter revealed that the incorporation of clay and MWNTs into ABS resin significantly reduced the peak heat release rate (PHRR) and slowed down the whole combustion process compared to the individual filled system based on clay or MWNTs. The flame retardancy of polymer nanocomposites is strongly affected by the formation of a network structure. The coexistence of clay and MWNTs in the composites can form a more effective confined space and enhances the network structure, which can be responsible for the improved flame retardancy for polymer nanocomposites in this study. The complex viscosity increases significantly with the addition of clay and MWNTs at higher temperature. For ABS/clay/MWNTs nanocomposites, the complex viscosity increases by at least one order when the temperature is higher than 240 °C than pure ABS resin. Because coexistence of clay and MWNTs can form more effective confined geometry, the ABS/clay/MWNTs nanocomposite can form network structure in lower temperature and protect the polymer matrix more efficiently.

The addition of MWNTs improves the basal spacing and the dispersion of clay layers in nanocomposites. MWNTs were shortened after combustion and there is no significant change for diameters. For chars of ABS/clay/MWNTs nanocomposites, some MWNTs run across between clay layers, which indicate a strong interaction between clay and MWNTs. The existence of clay enhances the graphitization degree of MWNTs during combustion. Clay can assist the elimination of dislocations and defects and the rearrangement of crystallites. Al<sub>2</sub>O<sub>3</sub>, one of the components of clay, acts as the catalyst of graphitization.

#### Acknowledgments

The authors are grateful to Professor Xiaobin Zhang and his research group at the Institute of Material Physics and Microstructure at Zhejiang University, for their graciously provided MWNTs. Financial support from the National Natural Science Foundation of China is also acknowledged.

#### References

- [1] Jia Z J, Wang Z Y, Xu C L, Liang J, Wei B C, Wu D H and Zhang Z M 2000 *J. Tsinghua Univ. (SCI and Tech)* **40** 14
- [2] Zhang W, Shen L, Phang I and Liu T 2004 *Macromolecules* **37** 256
- [3] Xia H S, Wang Q and Qiu G H 2003 *Chem. Mater.* **15** 3879
- [4] Liu T X, Phang I Y, Shen L, Chow S Y and Zhang W D 2004 *Macromolecules* **37** 7214
- [5] Thostenson E T, Ren Z and Chou T 2001 *Comput. Sci. Technol.* **1** 1899
- [6] Kashiwagi T, Gruke E, Hilding J, Groth K, Harris R, Butler K, Shields J, Kharchenko S and Douglas J 2004 *Polym. Degrad. Stab.* **45** 4227
- [7] Kashiwagi T, Gruke E, Hilding J, Groth K, Harris R, Awad W and Douglas J 2002 *Macromol. Rapid Commun.* **23** 761
- [8] Kashiwagi T, Du F, Winey K I, Groth K M, Shields J R, Bellayer S P, Kim H and Douglas J F 2005 *Polymer* **45** 471
- [9] Kashiwagi T, Du F, Douglas J F, Winey K I, Harris R H and Shields J R 2005 *Nat. Mater.* **4** 928
- [10] Schartel B, Potschke P, Knoll U and Goad M A 2005 *Eur. Polym. J.* **41** 1061
- [11] Pandey J K, Reddy K R, Kumar A P and Singh R P 2005 *Polym. Degrad. Stab.* **88** 234
- [12] Giannelis E P 1996 *Adv. Mater.* **8** 29
- [13] Zhu J and Wilkie C A 2000 *Polym. Intern.* **49** 1158
- [14] Tidjani A and Wilkie C A 2001 *Polym. Degrad. Stab.* **74** 33
- [15] Messersmith P B and Giannelis E P 1995 *J. Polym. Sci. A* **33** 1047
- [16] Morgan A B 2006 *Polym. Adv. Technol.* **17** 206
- [17] Serge Bourbigot S, Duquesne S and Jama C 2006 *Macromol. Symp.* **233** 180
- [18] Okoshi M and Nishizawa H 2004 *Fire Mater.* **28** 42
- [19] Beyer G 2002 *Fire Mater.* **26** 291
- [20] Gao F G, Beyer G and Yuan Q C 2005 *Polym. Degrad. Stab.* **89** 559
- [21] Peeterbroeck S et al 2004 *Compos. Sci. Technol.* **64** 2317
- [22] Beyer G 2005 *Fire Mater.* **29** 61
- [23] Peeterbroeck S, Alexandre M, Nagy J B, Moreau N, Destree A, Monteverde F, Rulmont A, Sporken R, Beyer G and Dubois P 2005 *Macromol. Symp.* **221** 115
- [24] Thomas C R 1993 *Essentials of Carbon–Carbon Composites* (Cambridge: Royal Society of Chemistry) p 33
- [25] Gong Q M, Li Z, Zhang Z Y, Wu B, Zhou X W, Huang Q Z and Liang J 2006 *Tribol. Int.* **39** 937

- [26] Cheng J P, Zhang X B, Luo Z Q, Liu F, Ye Y, Yin W Z, Liu W and Han Y X 2006 *Mater. Chem. Phys.* **95** 5
- [27] Cullity B D 1978 *Elements of X-ray diffraction* (New York: Addison-Wesley) p 142
- [28] Maire J and Mering J 1970 *Chem. Phys. Carbon* **6** 125
- [29] Dasgupta K and Sathiyamoorthy D 2003 *Mater. Sci. Technol.* **19** 995
- [30] Ma H Y, Fang Z P and Tong L F 2006 *Polym. Degrad. Stab.* **91** 1972
- [31] Krishnamoorti R and Silva A S 2000 *Polymer-clay nanocomposites* (New York: Wiley) pp 315–43
- [32] Ren J, Casanueva B F, Mitchell C A and Krishnamoorti R 2003 *Macromolecules* **36** 4188
- [33] Kim T H, Jang L W, Lee D C, Choi H J and Jhon M 2002 *Macromol. Rapid Commun.* **23** 191
- [34] Zhong Y, Zhu Z and Wang S Q 2005 *Polymer* **46** 3006
- [35] Wagener R and Reisinger T 2003 *Polymer* **44** 7513
- [36] Lee J A, Kontopoulou M and Parent J S 2004 *Polymer* **45** 6595
- [37] Du F, Scogna R C, Zhou W, Brand S, Fischer J E and Winey K I 2004 *Macromolecules* **37** 9048
- [38] Kim J A, Seong D G, Kang T J and Youn J R 2006 *Carbon* **44** 1898
- [39] Sung Y T, Han M S, Song K H, Jung J W, Lee H S, Kum C K, Joo J and Kim W N 2006 *Polymer* **47** 4434
- [40] Zou L H, Huang B Y, Huang Y, Huang Q Z and Wang C A 2003 *Mater. Chem. Phys.* **82** 654
- [41] Gong Q M, Li Z, Li D, Bai X D and Liang J 2004 *Solid State Commun.* **131** 399
- [42] Franklin R E 1951 *Acta. Crystallogr.* **4** 253
- [43] Rao A M *et al* 1997 *Science* **275** 187
- [44] Zhang F Q, Huang Q Z, Huang B Y, Gong Q M, Chen T F and Xiong X 2003 *J. Inorg. Mater.* **2** 361
- [45] Oya A and Otani S 1979 *Carbon* **17** 31
- [46] Oya A and Otani S 1979 *Carbon* **19** 391
- [47] Yu J K, Ueno S, Li H X and Hiragushi K 1999 *J. Eur. Ceram. Soc.* **19** 2843
- [48] Ahmadi S J, Huang U D and Li W 2004 *J. Mater. Sci.* **39** 1919